

Uncertainty in global CCN concentrations from uncertain aerosol nucleation and primary emission rates

J. R. Pierce^{1,*} and P. J. Adams¹

¹Center for Atmospheric Particle Studies, Carnegie Mellon Univ., Pittsburgh, PA, USA

* now at: Goddard Space Flight Center, Greenbelt, MD, USA, 20771, USA

Received: 21 July 2008 – Published in Atmos. Chem. Phys. Discuss.: 26 August 2008

Revised: 26 January 2009 – Accepted: 6 February 2009 – Published: 19 February 2009

Abstract. The indirect effect of aerosols on climate is highly uncertain and limits our ability to assess anthropogenic climate change. The foundation of this uncertainty is uncertainty in the number of cloud condensation nuclei (CCN), which itself stems from uncertainty in aerosol nucleation, primary emission and growth rates. In this paper, we use a global general circulation model with aerosol microphysics to assess how the uncertainties in aerosol nucleation, emission and growth rates affect our prediction of CCN(0.2%) concentrations. Using several nucleation rate parameterizations that span six orders of magnitude of globally averaged nucleation rates, the tropospheric average CCN(0.2%) concentrations vary by 17% and the boundary layer average vary by 12%. This sensitivity of tropospheric average CCN(0.2%) to the nucleation parameterizations increases to 33% and 20% when the total primary emissions are reduced by a factor of 3 and the SOA condensation rates are increased by a factor of 3.5, respectively. These results show that it is necessary to better understand global nucleation rates when determining CCN concentrations. When primary emissions rates are varied by a factor of 3 while using a binary nucleation parameterization, tropospheric average CCN(0.2%) concentrations also vary by 17%, but boundary layer average vary by 40%. Using the fastest nucleation rate parameterization, these changes drop to 3% and 22%, respectively. These results show the importance of reducing uncertainties in primary emissions, which appear from these results to be somewhat more important for CCN than the much larger uncertainties in nucleation. These results also show that uncertainties in nucleation and primary emissions are more important when sufficient condensable material is available to

grow them to CCN sizes. The percent change in CCN(0.2%) concentration between pre-industrial times and present day does not depend greatly on the nucleation rate parameterization used for our base case scenarios; however, because other factors, such as primary emissions and SOA, are uncertain in both time periods, this may be a coincidence.

1 Introduction

Atmospheric aerosols are important to climate because they scatter and absorb radiation and affect the radiative properties of clouds. The connections between aerosols and cloud radiative properties are known as the indirect effects of aerosols on climate. The aerosol indirect effects occur because anthropogenic emissions have increased the number of cloud condensation nuclei (CCN), the particles on which cloud drops form. The first indirect effect, or cloud albedo effect, occurs because the reflectivity of sunlight (albedo) in a cloud is modified by changes in cloud droplet number concentration (CDNC). With constant cloud liquid water mass, increases in CCN/CDNC cause increases in liquid water surface area, thus reflecting more sunlight to space and cooling climate (Twomey, 1974, 1977, 1991). In the Intergovernmental Panel on Climate Change (IPCC) Fourth Assessment Report, the cloud albedo effect was the most uncertain of the quantified radiative forcing changes since pre-industrial times. The estimated albedo effect spanned -0.3 to -1.8 W m^{-2} (Forster et al., 2007). The second indirect effect, or cloud lifetime effect, occurs because increasing the CDNC reduces the diameter of the cloud droplets (Albrecht, 1989) inhibiting the cloud's ability to precipitate. However, potential cloud-dynamic feedbacks complicate the calculation of this effect (Ackerman et al., 2004; Twohy et al.,



Correspondence to: J. R. Pierce
(jeffrey.robert.pierce@gmail.com)

2005). The IPCC has not quantified the value of radiative forcing from the cloud lifetime effect. It is necessary to understand the causes of these large aerosol-cloud-climate uncertainties in order to reduce these large uncertainties.

In order to quantify how clouds have changed, the change in CCN concentrations due to human activity must be understood. Whether or not an atmospheric particle will act as a CCN depends on the maximum water-vapor supersaturation in the clouds along with the diameter and composition of the particle. In typical stratus clouds with a maximum supersaturation of about 0.2%, particles with dry diameters larger than about 80–100 nm generally act as CCN. All particles in the atmosphere are either emitted directly to the atmosphere as a particle (primary emissions) or are formed in-situ in the atmosphere from condensable gases (particle nucleation or new particle formation). CCN may either be emitted directly at CCN sizes, have grown from a primary particle smaller than CCN sizes or have grown from a nucleated particle. It has been proposed that in many parts of the atmosphere, nucleation and subsequent growth to CCN sizes is a dominant pathway for the formation of CCN (Pirjola et al., 2002; Lihavainen et al., 2003; Laaksonen et al., 2005; Sotiropoulou et al., 2006), while in other areas, particularly in the boundary layer and near particle sources, primary emissions dominate CCN production (Adams and Seinfeld, 2003; Spracklen et al., 2005b; Pierce and Adams, 2006). Therefore, uncertainty in aerosol nucleation rates and primary emission rates and sizes may lead to large uncertainties in predicted CCN concentrations.

There are several proposed particle nucleation mechanisms that may be significant for particle formation globally. These mechanisms include: binary nucleation in which sulfuric acid vapor and water vapor condense to form the new particles (Jacker-Voirol and Mirabel, 1989; Kulmala et al., 1998; Vehkamäki et al., 2002), ternary nucleation in which sulfuric acid vapor, ammonia and water vapor condense to form the new particles (Kulmala et al., 2002; Napari et al., 2002; Anttila et al., 2005; Yu, 2006b) and ion-induced nucleation in which gas-phase ions aid in either binary or ternary nucleation (Yu and Turco, 2001; Laakso et al., 2002; Kazil and Lovejoy, 2004; Lovejoy et al., 2004; Kazil et al., 2006; Yu, 2006a). Additionally, cluster activation theory has been proposed to explain the dependence of nucleation rate on sulfuric acid concentrations in the boundary layer (Kulmala et al., 2006; Sihto et al., 2006). Depending on the nucleation mechanism or model of the nucleation mechanism, the predicted nucleation rates may differ by many orders of magnitude (Lucas and Akimoto, 2006; Jung et al., 2008). Globally, Lucas and Akimoto (2006) showed that the maximum nucleation rates varied by five orders of magnitude between the Vehkamäki et al. (2002) binary nucleation parameterization, Napari et al. (2002) ternary nucleation parameterization, and Modgil et al. (2005) ion-induced nucleation parameterization.

The ability for new particles to grow to CCN sizes depends on the existing size distribution of particles and the condensational growth rate of the new particle (Pierce and Adams, 2007). This means that the sensitivity of CCN to nucleation rates will depend greatly on the factors that control the size distribution (e.g. the primary emissions size and rate, the condensation rate and the nucleation rate itself) and growth rate (e.g. the SOA and sulfate condensation rates and the size distribution). Furthermore, because the size distributions and condensational growth rates have changed between pre-industrial times and today, the sensitivity of CCN to nucleation rates may also have changed.

Emitted particles mix into the atmosphere at sizes generally much larger (diameters at least 10 nm or greater) than the size of nucleated particles (diameters of ~ 1 nm). This means that emitted particles affect CCN concentrations more easily than do nucleated particles (Pierce and Adams, 2007). The uncertainties in the primary emission rates and sizes, although still large, are generally much smaller than the uncertainties in the nucleation rates; however, because these emitted particles affect CCN more efficiently than nucleated particles, they may also contribute greatly to uncertainty in CCN predictions. We will examine the relative importance of uncertainties in primary emissions and nucleation rates to CCN formation globally. This will allow resources to be directed at reducing the uncertainties of the more important process.

Recently, global atmospheric models with online aerosol microphysics have been used to predict the time and location dependent aerosol size distributions (Ghan et al., 2001; Wilson et al., 2001; Adams and Seinfeld, 2002; Adams and Seinfeld, 2003; Easter et al., 2004; Rodriguez and Dabdub, 2004; Spracklen et al., 2005b; Spracklen et al., 2005a; Stier et al., 2005; Pierce and Adams, 2006; Spracklen et al., 2006; Stier et al., 2006; Pierce et al., 2007; Spracklen et al., 2008). These models provide a tool for evaluating the connection between nucleation/emissions and the concentrations of CCN in the global atmosphere. Spracklen et al. (2006) evaluated the contribution of boundary layer nucleation from cluster activation theory to particle number in a global model and found that particle concentrations in remote continental regions are likely dominated by nucleated particles while concentrations in polluted continental regions are likely dominated by primary particles. Spracklen et al. (2008) expanded this work to explore the impact of these boundary layer nucleation events on boundary layer CCN as well as exploring the effect of uncertain SOA condensation rates on the connection between nucleation and CCN. Similarly, Makkonen et al. (2008) explored the sensitivity of aerosol and cloud droplet number concentrations to boundary layer nucleation rates and SOA formation rates. Both of these studies showed that CCN concentrations can vary by large amounts at some boundary layer locations due to changes in the nucleation and SOA rates. Complimenting these studies, Wang and Penner (2008) showed how the contribution of boundary layer nucleation to CCN depends greatly on the primary emissions rates in the

model. These important studies have shown that CCN predictions will remain uncertain until we have a better understanding on nucleation, primary emissions and SOA. However, there remains a gap in our understanding of the relative importance of each of these processes to predicting CCN. This relative importance is necessary to determine where future research should be focused in order to improve CCN estimates.

In this paper, we will use a global aerosol microphysics model (Adams and Seinfeld, 2002; Pierce and Adams, 2006; Pierce et al., 2007) to:

1. Evaluate the sensitivity of total particle number and CCN concentrations to nucleation rates.
2. Determine how the sensitivity of CCN to nucleation rates depends on other factors: SOA condensation rates and the primary emissions rates.
3. Compare the sensitivity of CCN to nucleation rates to the sensitivity of CCN to primary emissions rates.
4. Estimate how the sensitivity of CCN to nucleation may have changed since the pre-industrial time period.

The following section of the paper describes the model details and the various simulations. Section 3 describes the results and the conclusions are given in Sect. 4.

2 Model description

2.1 Overview

The simulations presented in this paper are performed in the Goddard Institute for Space Studies model II-prime (GISS II-prime) (Hansen et al., 1983; Prather, 1986; Del Genio and Yao, 1992; Del Genio et al., 1996; Rind and Lerner, 1996). The model resolution is 4 degrees latitude by 5 degrees longitude and has 9 vertical layers from the surface to the model top at 10 mb in the stratosphere, although the layers are concentrated in the troposphere. For the simulations here, the model is initialized for the first three modeled months. An additional 12 months of simulation are used for the results. All results shown in this paper are annually averaged over this year.

The aerosol size distribution between dry diameters 10 nm to 10 μm is represented using the Two-Moment Aerosol Sectional (TOMAS) microphysics algorithm (Adams and Seinfeld, 2002). The size distribution is divided into 30 geometrically spaced size sections classified by the mass of the particles without ammonium or water. The number of particles in each size section is predicted as well as the mass of aerosol sulfate, sea salt, hydrophilic organic matter, hydrophobic organic matter, internally-mixed elemental carbon and externally-mixed elemental carbon in each size section. Additionally, the mass of aerosol water in each size section,

total amount of aerosol ammonium and total aerosol MSA are also predicted for a total of 242 online aerosol tracers in each grid cell. Besides these aerosol species, the model also predicts the following six gas-phase species: H_2O_2 , SO_2 , DMS, H_2SO_4 , NH_3 and a generic gas representing secondary organic aerosol (SOA) precursors for a total of 248 tracked species. Size-resolved dry and wet deposition is as described in Pierce et al. (2007) and Adams and Seinfeld (2002). Modified Köhler theory (Raymond and Pandis, 2002; Raymond and Pandis, 2003) is used to determine the CCN(0.2%) concentrations throughout this paper as described in Pierce et al. (2007).

2.2 Changes to previous version of model

The model used here includes several modifications to the model used in Pierce et al. (2007). Nucleation and condensation rates are now calculated simultaneously using the pseudo-steady-state approximation (PSSA) for sulfuric acid vapor (Pierce and Adams, 2009). In general, this greatly increases the length of time steps allowed while still simulating accurately the nucleation rates, thus decreasing computation time. The accuracy and speed of the PSSA was evaluated in Pierce and Adams (2009). Rather than explicitly representing aerosol microphysics below 10 nm, the growth of nucleated particles to the first size bin ($D_p=10$ nm) is now approximated using the parameterization of Kerminen et al. (2004). This approximation predicts the formation of 10-nm particles from the formation rate of critical-nuclei-sized particles, the condensational growth rate of these particles and the total condensation sink of existing particles larger than 10 nm. The growth of the new particles to 10 nm occurs due to condensation of both sulfuric acid and SOA. The growth of the nuclei through self-coagulation is not considered leading to an underprediction of the 10 nm particle formation rate when the new particle formation rate is large (Kerminen et al., 2004). Errors from this technique also occur due to the instantaneous growth of nucleated clusters to 10-nm particles. This instantaneous growth assumes that the growth rate remains constant throughout the growth to 10 nm, such that changes in the growth rate would lead to errors. Additionally, errors may occur because the instantaneous growth to 10 nm will artificially increase the condensation sink earlier in the nucleation event.

Gas-phase ammonia and bulk aerosol ammonium are now simulated in the model in order to predict ternary nucleation rates. All ammonia is assumed to be aerosol ammonium when the total number of ammonia molecules (gas phase ammonia plus particle ammonium) is less than two times the total aerosol sulfate molecules. When the total number of ammonia molecules is greater than two times the total aerosol sulfate molecules, the excess ammonia is free gas-phase ammonia. The aerosol ammonium is assumed to partition to aerosol sizes in proportion to the sulfate mass. Realistically, gas-phase ammonia is present even when the aerosols are

acidic; therefore, our assumption about gas-phase ammonia being present only when sulfate is neutralized may lead to an underprediction of gas-phase ammonia and ternary nucleation rates. As will be discussed in the next section, ternary nucleation rates are already very high, and this underprediction does not likely affect the results. The emissions of ammonia will be discussed in a subsequent section.

In order to account for growth of particles from the condensation of SOA (Kulmala et al., 2005; Vaattovaara et al., 2006; Holmes, 2007), we have implemented a simple but flexible treatment of SOA formation. A generic SOA precursor representing all SOA precursor gases is emitted and forms SOA with a first-order loss rate of 12 h. The SOA precursor is assumed to convert entirely to SOA and is used to generate specific SOA condensation rates. This does not represent any actual SOA precursor in the atmosphere; however, this allows us to control easily how much SOA condenses onto the particles globally. The condensed SOA is treated as non-volatile hydrophilic organic matter as described in Pierce et al. (2007). The SOA condenses onto the aerosol size distribution in proportion to its effective surface area (corrected for non-continuum effects). This assumption regarding the condensation of SOA is consistent with the fact that growth of nucleation-mode particles is often dominated by the condensation of organics (Fan et al., 2006; Laaksonen et al., 2008). The SOA fields will be discussed further in the emissions section.

The number median diameter of biomass burning and biofuel burning carbonaceous emissions has been increased from 30 nm to 100 nm based on measurements from biomass burning plumes in the Amazon (Rissler et al., 2004; Rissler et al., 2006). Fossil fuel primary carbonaceous emissions are still emitted with a number median diameter of 30 nm. Primary sulfate aerosol emissions have been reduced from 3% of aerosol sulfur emissions to 1% of aerosol sulfur emissions because the model was overpredicting the measured number of particles in polluted regions even when carbonaceous aerosols were omitted. Additionally, to account for sub-grid coagulation, the simulations now include the parameterization of Pierce et al. (2008), which aids in predicting regional background concentrations. In this implementation of the parameterization, primary particles undergo coagulation with pre-existing particles for 10 h to determine their “effective” regional emissions size and number distributions.

2.3 Nucleation mechanisms

Three nucleation rate parameterizations are used in these simulations, the binary nucleation parameterization of Vehkamäki et al. (2002), the ternary nucleation parameterization of Napari et al. (2002) and the cluster activation parameterization of Kulmala et al. (2006). The Vehkamäki et al. (2002) binary nucleation has a moderate nucleation rate that occurs primarily in the free troposphere, whereas the Napari et al. (2002) ternary nucleation has very high nucleation

rates that occur throughout the entire troposphere (Lucas and Akimoto, 2006). The first two parameterizations will be used here to estimate potential bounds on the effect of nucleation on CCN. When gas-phase ammonia is present, the Napari et al. (2002) parameterization predicts nucleation rates many orders of magnitude faster than the Vehkamäki et al. (2002). In the simulations using Napari et al. (2002), the Vehkamäki et al. (2002) parameterization is used when gas-phase ammonia concentrations are below 0.1 pptv. There are several issues with employing the Napari et al. (2002) parameterization in this work. One is that the ammonia input into the parameterization is a mixing ratio rather than a concentration. Because the nucleation rate should depend on the ammonia concentration, not its mixing ratio, we convert the ammonia to an effective mixing ratio defined as the ammonia mixing ratio at 273 K and 1 atm if the ammonia concentration were held constant. Another issue is that it has been shown that Napari et al. (2002) yields nucleation rates that are unrealistically high (Anttila et al., 2005; Gaydos et al., 2005; Jung et al., 2006; Merikanto et al., 2007). Merikanto et al. (2007) presents a parameterization of ternary nucleation that includes the effect of stable ammonium bisulfate formation that was not included in Napari et al. (2002). The Merikanto et al. (2007) parameterization, however, predicts nucleation rates in our model similar to that of Vehkamäki et al. (2002). The fact that the Napari et al. (2002) parameterization better predicts boundary layer nucleation events (or lack thereof) in Pittsburgh than six other parameterizations considered, including Merikanto et al. (2007), suggests that it has skill in predicting atmospheric nucleation occurrences in the Northeastern United States (Jung, 2008; Jung et al., 2008). Because we are concerned in this paper with the sensitivity of CCN to large potential uncertainties nucleation, we continue to use the Napari et al. (2002) parameterization. A third issue with using the Napari et al. (2002) parameterization (or any parameterization that predicts very high nucleation rates) is that it predicts nucleation rates fast enough that nucleation mode growth through self coagulation is important. The nucleation-mode parameterization of Kerminen et al. (2004) does not take into account self coagulation, so the new particle formation rate at 10 nm diameter may be underpredicted in cases where self coagulation is the primary growth mechanism for nucleation-mode particles. Due to the large uncertainty in the ternary nucleation rates, we present additional results from a simulation that uses the Vehkamäki et al. (2002) parameterization in the free troposphere and additionally use the cluster activation-type nucleation in the boundary layer (Kulmala et al., 2008). The nucleation rate of 1 nm clusters are proportional to the gas-phase sulfuric acid concentration, and the proportionality constant is $1.0 \times 10^{-6} \text{ s}^{-1}$ (Sihto et al., 2006). The simulation using the activation-type nucleation in the boundary layer will give enhanced boundary layer nucleation, but with rates more likely realistic than the ternary nucleation simulations.

2.4 Emissions

In the simulations, we investigate the implications of various assumptions about present-day and pre-industrial gas and aerosol emissions as well as varying SOA production rates.

2.4.1 Present-day emissions

The present-day sulfur (SO_2 and DMS) emissions are described in detail in Koch et al. (1999). The DMS emissions total $10.8 \text{ Tg S yr}^{-1}$. The volcanic emission rate of SO_2 is 4.8 Tg S yr^{-1} . The emission rate of anthropogenic SO_2 is $68.3 \text{ Tg S yr}^{-1}$. One percent of anthropogenic sulfur emissions are emitted as primary sulfate (0.7 Tg S yr^{-1}). The primary sulfate is emitted in two modes. Fifteen percent of the mass is emitted to the first mode, which has a number median diameter of 10 nm and a geometric standard deviation of 1.6. The remainder of the mass is in the second mode, which has a number median diameter of 70 nm and a geometric standard deviation of 2 (Adams and Seinfeld, 2002; Adams and Seinfeld, 2003). The total emission rate of ammonia is $57.6 \text{ Tg N yr}^{-1}$ (Bouwman et al., 1997; Adams et al., 1999; Adams et al., 2001). Because the same host model is used, the resultant ammonia and ammonium concentration fields are close to those in Adams et al. (1999). The emissions of carbonaceous aerosol are the same as the BBASE simulation in Pierce et al. (2007) except for the change in the size of emissions for open burning and biofuel burning as described in Sect. 2.2. These primary organic and elemental carbon aerosol emissions rates are taken from Bond et al. (2004). We add seasonality to the Bond et al. (2004) open burning emissions by scaling the emissions to the fractions of the grid cells that are on fire as used by Liousse et al. (1996), while keeping the total annual emissions from open burning constant. To convert the organic carbon (OC) mass presented in Bond et al. (2004) to OM we assume an OM:OC ratio of 1.8 (El-Zanan et al., 2005; Yu et al., 2005; Zhang et al., 2005). The emissions rates of OM and EC are 61 Tg yr^{-1} and 8.0 Tg yr^{-1} , respectively. Sea-salt emissions are found using the emissions parameterization of Clarke et al. (2006) and is described in Pierce and Adams (2006). The resulting sea-salt mass emission rate is 7120 Tg yr^{-1} .

SOA is generated from biogenic and a generic “additional/anthropogenic” sources. The biogenic SOA source is from SOA fields given in the AEROCOM inventory (Dentener et al., 2006). The biogenic SOA leads to 19.1 Tg yr^{-1} of SOA condensed. The biogenic SOA formation alone is within the lower end of the estimate for global SOA ($12\text{--}70 \text{ Tg yr}^{-1}$) given in Kanakidou et al. (2005). In certain simulations, an additional source of SOA precursor is emitted to determine an upper bound on the contribution of SOA to the growth of ultrafine particles to CCN. The sources of these emissions are assumed to be co-located with anthropogenic SO_2 emissions and contribute an additional 45 Tg yr^{-1} net condensation of SOA. Because regions near anthropogenic

SO_2 sources are often rich with ultrafine particles, we expect that emitting the additional SOA in these regions will maximize the increase the number of CCN, thereby achieving an upper bound on SOA contribution to CCN. We refer to this SOA source as “additional SOA”. The combined SOA is close to the upper bound of the estimate in Kanakidou et al. (2005).

2.4.2 Pre-industrial emissions

Pre-industrial sea-salt, DMS and volcanic SO_2 emissions are the same as in the present-day simulations. SO_2 emissions from domestic and open biomass burning for the year 1750 are taken from the AEROCOM inventory and are 1.6 Tg yr^{-1} (Dentener et al., 2006). No sulfur is emitted as primary sulfate. The pre-industrial ammonia emissions are described in Adams et al. (2001) and the total emission rate of ammonia is $18.7 \text{ Tg N yr}^{-1}$. The pre-industrial fossil fuel contribution to carbonaceous emissions is assumed to be zero. The pre-industrial open burning and biofuel contributions to carbonaceous emissions are taken for the year 1750 from the AEROCOM inventory (Dentener et al., 2006). The emissions rates of OM and EC are 30 Tg yr^{-1} and 1.4 Tg yr^{-1} , respectively. The number median diameter for these emissions is 100 nm with a geometric standard deviation of 2 as with the present day simulations. All pre-industrial simulations use the same biogenic SOA as in the present-day simulations but do not include the “additional SOA” source.

2.5 Simulations

Table 1 summarizes the ten simulations that will be discussed in this paper. The NONUC simulation uses the standard present-day gas and aerosol emissions, includes biogenic SOA, but has no nucleation. NONUC is used as a baseline for assessing the contribution of nucleation to CCN. The BINARY and TERNARY simulations are similar, but use the Vehkamäki et al. (2002) and Napari et al. (2002) nucleation parameterizations, respectively. These two simulations are compared to see how the choice of nucleation parameterization may affect the CCN prediction with our base-case present-day emissions and SOA. The REDBINARY (reduced binary nucleation) simulation is the same as the BINARY simulation except the binary nucleation rates predicted by Vehkamäki et al. (2002) are reduced by a factor of ten. The ACTIVATION simulation is the same as BINARY, except the cluster activation-type nucleation scheme of Kulmala et al. (2006) is used to predict the nucleation rates within the boundary layer (the results for this simulation are only for the month of June). The REDBINARY and ACTIVATION simulations give further insight into how sensitive CCN predictions are due to more modest changes in nucleation rate. The BINARY-RP and TERNARY-RP (reduced primary emissions) simulations are the same as the BINARY and TERNARY simulations except that the aerosol

Table 1. Overview of simulations. Detailed descriptions of the nucleation parameterizations, emissions and SOA treatments are in the text.

Name	Nucleation parameterization	Primary aerosol emissions	SO ₂ and NH ₃	SOA
NONUC	none	Present	Present	Base
BINARY	Vehkamäki et al. (2002)	Present	Present	Base
TERNARY	Napari et al. (2002)	Present	Present	Base
REDBINARY	Vehkamäki et al. (2002)	Present	Present	Base
ACTIVATION*	Sihto et al. (2006) and Vehkamäki et al. (2002)	Present	Present	Base
BINARY-RP	Vehkamäki et al. (2002)	Present/3	Present	Base
TERNARY-RP	Napari et al. (2002)	Present/3	Present	Base
BINARY-HISOA	Vehkamäki et al. (2002)	Present	Present	Enhanced
TERNARY-HISOA	Napari et al. (2002)	Present	Present	Enhanced
BINARY-PI	Vehkamäki et al. (2002)	Pre-industrial	Pre-industrial	Base
TERNARY-PI	Napari et al. (2002)	Pre-industrial	Pre-industrial	Base

* Activation-type nucleation in boundary layer and binary homogeneous nucleation in free troposphere; results only for the month of June

primary emissions (both number and mass of all natural and anthropogenic emissions) are reduced by a factor of 3. The factor of 3 reduction was chosen to represent the variability generally found in emissions inventories (Penner et al., 2001). This allows us to calculate the sensitivity of CCN to changes in primary emissions and determine how much more sensitive CCN concentrations are to nucleation when fewer primary emissions are present. The BINARY-HISOA and TERNARY-HISOA (high SOA) simulations are the same as the BINARY and TERNARY simulations except that “additional SOA” described above is included. These simulations are used to explore how the sensitivity of CCN to nucleation rates depends on the growth rates of the new particles. The BINARY-PI and TERNARY-PI simulations use the pre-industrial gas and aerosol emissions. These simulations are used to determine if the sensitivity of CCN to nucleation rate changes between the pre-industrial time period and today.

3 Results

3.1 Aerosol number budgets

Annually averaged aerosol number budgets for ten simulations are shown in Table 2. Values for BINARY, TERNARY and ACTIVATION are also shown for the month of June. Shown are the global nucleation rate, new particle formation rate into the first model bin (~ 10 nm), primary emissions rate, the total number of particles with $D_p > 10$ nm (condensation nuclei, CN₁₀) and the total number of CCN at 0.2% supersaturation (CCN(0.2%)). For ease of interpretation, all values in the table are normalized by the volume of the troposphere at 273 K and 1 atm. In the final column is what we call the Number Utilization Efficiency (NUE). The NUE is defined as:

$$\text{NUE} = \frac{\left(\frac{\text{CCN}}{\tau_{\text{CCN}}}\right)}{E+J} \quad (1)$$

where CCN is the total number of CCN in the atmosphere, τ_{CCN} is the lifetime of CCN (approximated here to be 7 days), E is the global particle number emission rate and J is the global particle nucleation rate. The NUE is the global average fraction of new particles that form CCN. The NUE is many orders of magnitude smaller in the ternary nucleation simulations indicating the very low probability of growth to CCN sizes when many nuclei are present. Table 2 will be referenced throughout the paper as we explore the simulations in detail.

The difference between the nucleation rate and the new particle formation rate at 10 nm highlights the effect of the Kerminen et al. (2004) parameterization that approximates the new particle formation rate at 10 nm from the nucleation rate, growth rate and condensation sink. Note that the predicted nucleation rates are about six orders of magnitude apart between corresponding binary and ternary nucleation simulations, but the difference in the new particle formation rates at 10 nm are only about an order of magnitude apart. Similarly, for the June results, the ACTIVATION simulation has tropospheric nucleation rates about 8 times larger than BINARY; however, their 10 nm formation rates are only a factor of 2 apart. This strong dampening of the 10 nm new particle formation rate to changes in the nucleation rate results from a combination of three factors: slower condensational growth rates at faster nucleation rates due to larger condensation sinks, faster coagulation removal rates at faster nucleation rates due to larger coagulation sinks and the lack of growth through nucleation-mode self coagulation in the Kerminen et al. (2004) parameterization. The first two effects are realistic, but the latter effect is due to a limitation of the parameterization. It is difficult at this time to determine how much of the dampening is from each of these effects.

Table 2. Global annual-average tropospheric aerosol number budgets and burdens for the various simulations. Values normalized by tropospheric volume at 273 K and 1 atm.

Name	Nucleation rate ($\text{cm}^{-3} \text{s}^{-1}$)	New particle formation rate at 10 nm($\text{cm}^{-3} \text{s}^{-1}$)	Emission rate ($\text{cm}^{-3} \text{s}^{-1}$)	CN($D_p > 10 \text{ nm}$) cm^{-3}	CCN(0.2%) cm^{-3}	NUE*
NONUC	0.00×10^0	0.00×10^0	1.09×10^{-3}	254	116	1.8×10^{-1}
BINARY	5.77×10^{-3}	3.74×10^{-4}	1.09×10^{-3}	545	143	3.5×10^{-2}
TERNARY	1.01×10^4	9.18×10^{-3}	1.09×10^{-3}	1350	167	2.7×10^{-8}
REDBINARY	1.21×10^{-3}	1.94×10^{-4}	1.09×10^{-3}	443	139	1.0×10^{-1}
BINARY-RP	6.38×10^{-3}	4.54×10^{-4}	3.71×10^{-4}	489	122	3.0×10^{-2}
TERNARY-RP	1.04×10^4	1.04×10^{-2}	3.71×10^{-4}	1400	162	2.6×10^{-8}
BINARY-HISOA	4.01×10^{-3}	2.79×10^{-4}	1.09×10^{-3}	489	159	5.2×10^{-2}
TERNARY-HISOA	9.22×10^3	1.03×10^{-2}	1.09×10^{-3}	1270	190	3.4×10^{-8}
BINARY-PI	6.27×10^{-4}	1.67×10^{-4}	6.00×10^{-5}	272	45.1	1.1×10^{-1}
TERNARY-PI	2.08×10^3	1.14×10^{-2}	6.00×10^{-5}	807	55.8	4.4×10^{-8}
BINARY (June)**	4.82×10^{-3}	4.35×10^{-4}	1.09×10^{-3}	589	174	4.9×10^{-2}
TERNARY (June)**	1.25×10^4	9.96×10^{-3}	1.09×10^{-3}	1552	210	2.8×10^{-8}
ACTIVATION (June)**	3.66×10^{-2}	9.31×10^{-4}	1.09×10^{-3}	685	183	8.0×10^{-3}

* NUE, Number Utilization Efficiency, is the fraction of nucleated and emitted particles that become a CCN

** Data for month of June only

3.2 Comparison of aerosol number to observations

In order to address the sensitivity of aerosol budgets to nucleation, primary emissions and SOA, we must verify that our model is getting atmospherically relevant results. We compare the annually averaged CN ($D_p > 10 \text{ nm}$, CN10) concentrations to observations of annually averaged CN10 from the locations in Table 3 and Fig. 1 (note, ACTIVATION results are not presented here because we do not have a full year of data). The data we have chosen was restricted to sites outside urban areas with a minimum sample time of about one year. The sites included are part of a European network of sites presented in Van Dingenen et al. (2004), the Global Monitoring Division (GMD) of the Earth Systems Research Laboratory (Schnell, 2003; <http://www.esrl.noaa.gov/gmd/>) and the Thompson Farm site of AIRMAP (<http://airmap.unh.edu/>). The CN10 observations were taken using a condensation nucleus counter (CNC) in the case of the GMD and AIRMAP data and using a CNC with various size scanning devices in the case of the European sites. The low diameter cutoff for the CNCs in the GMD and AIRMAP data is 10 nm (which corresponds to the lower size limit of the model). The lower size limit for the CNCs used in the Van Dingenen et al. (2004) paper vary, however, they have corrected their number counts for a lower cutoff of 10 nm using the size-distribution measurements. The anthropogenic SO_2 emissions for the model are taken from the 1985 GEIA emissions inventory. Because these emissions have generally decreased since 1985 in Europe and North America where most of the comparisons are located, the modeled CN10 may be biased

high in these locations. This bias, along with the difficulty in comparing point concentration measurements to predicted concentrations in large grid boxes, prevents us from making any hard conclusions regarding the accuracy of individual simulations. Furthermore, even if we did not have any bias or sampling issues, the model could be tuned to match the observations through many different combinations of nucleation, primary emissions and SOA, making it impossible in a CN-only comparison to know which combination is correct. Regardless, these comparisons allow us to make sure that we are generally predicting atmospherically relevant concentrations and that we do not have major microphysical errors in the model.

The log-mean normalized bias (LMNB) and log-mean normalized error (LMNE) for the comparisons are included on each panel. The LMNB for the various simulations range from -0.04 to 0.43 , meaning that the average bias in the simulations range from an underprediction of 9% to an overprediction of a factor of 2.7. The LMNE for the various simulations range from 0.27 to 0.44, meaning that the average error in the simulations range from a factor of 1.9 to a factor of 2.7. These values shown here show a large improvement, particularly in the bias, over the same comparison in Pierce et al. (2007). The most similar simulation in Pierce et al. (2007) to those shown here, BBASE, had a LMNB of 0.68 and a LMNE of 0.70 corresponding to overpredictions by an average factor of 4.8. The improvements in the simulations shown in this paper are due to the reduction of the fraction of primary sulfate emissions from 3% of anthropogenic sulfur to 1%, the increase in the size of open burning

Table 3. Locations of number concentration measurements used for comparison. CN is the number of particles with diameter larger than 10 nm.

	Location	Region	Reference	Time	Lat.	Lon.	Elev.(m)	CN(cm ⁻³)
A	Aspvereten, Sweden	Europe	Van Dingenen et al. (2004)	Jan 2001–Dec 2001	58.8°	69.4°	20	2000
B	Harwell, UK	Europe	Van Dingenen et al. (2004)	May 1998–Nov 2000	51.6°	−1.3°	125	3000
C	Hohenpeissenberg, Germany	Europe	Van Dingenen et al. (2004)	Apr 1998–Aug 2000	47.8°	11.0°	988	2500
D	Melpitz, Germany	Europe	Van Dingenen et al. (2004)	Dec 1996–Nov 1997	51.5°	12.9°	86	5600
E	Ispra, Italy	Europe	Van Dingenen et al. (2004)	Feb 2000–Dec 2000	45.8°	8.6°	209	9000
F	Thompson Farm, NH, USA	North America	http://www.airmap.unh.edu	2001–2005	43.1°	−71.0°	75	7250
G	Lamont, OK, USA	North America	http://www.cmdl.noaa.gov/aero/data/	1996–2004	36.5°	−97.5°	318	5200
H	Bondville, IL, USA	North America	http://www.cmdl.noaa.gov/aero/data/	1994–2005	40.1°	−88.3°	230	3700
I	Sable Island, NS, Canada	North America	http://www.cmdl.noaa.gov/aero/data/	1992–1999	43.9°	−60.0°	5	850
J	Trinidad Head, CA, USA	North America	http://www.cmdl.noaa.gov/aero/data/	2002–2005	41.1°	−124.2°	107	590
K	American Samoa, USA	Remote	http://www.cmdl.noaa.gov/aero/data/	1995–2005	−14.2°	−170.5°	42	220
L	South Pole	Remote	http://www.cmdl.noaa.gov/aero/data/	1995–2005	−90.0°	102.0°	2810	100
M	Point Barrow, AK, USA	Remote	http://www.cmdl.noaa.gov/aero/data/	1995–2005	71.3°	−156.6°	11	110
N	Mauna Loa, HI, USA	Free Troposphere	http://www.cmdl.noaa.gov/aero/data/	1995–2005	19.5°	−155.6°	3397	330
O	Jungfraujoch, Switzerland	Free Troposphere	Van Dingenen et al. (2004)	Jun 1997–May 1998	47.6°	8.0°	3580	525

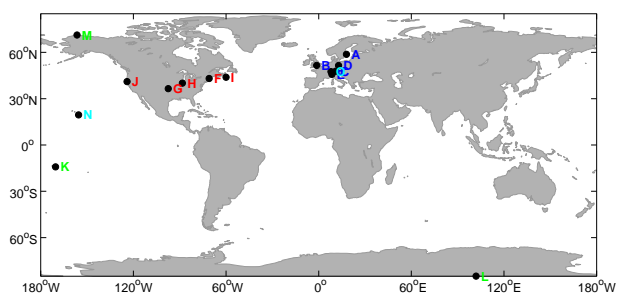


Fig. 1. Locations of aerosol number concentration measurements used for model evaluation. Letters correspond to those listed in Table 3, which provides additional details. Dark blue letters denote European boundary layer, red letters denote polluted North American boundary layer, green letters denote remote boundary layer, and cyan letters denote free troposphere.

and biofuel combustion carbonaceous emissions and the addition of the sub-grid coagulation parameterization Pierce et al. (2008). Of course as we noted previously, there are many ways to improve the comparison to these measurements. In the case of the carbonaceous emissions and sub-grid coagulation, however, these changes were based on independent improvements in the understanding of the emissions (Rissler et al., 2004, 2006) and theory (Pierce et al., 2008).

In general, the most important factor affecting these comparisons is whether the simulations used the nucleation schemes of Vehkamäki et al. (2002) or Napari et al. (2002) (the binary and ternary simulation families). The simulated CN₁₀ is markedly different between the pairs of binary and ternary simulations (holding everything else constant). However, the omission of nucleation altogether (NONUC), compared to the BINARY case, only affected the CN₁₀ at some of the most remote locations. The reduction of primary emissions caused a large change in the simulated CN₁₀ only when

binary nucleation was used (BINARY versus BINARY-RP). For the same reduction of primary emissions in the ternary cases, the comparison was insensitive to the primary emissions due to a saturation of CN₁₀ in the boundary layer by nucleation. Increasing SOA only slightly affected the comparisons. Additional SOA acts to both increase the coagulation sink (reducing the predicted CN₁₀) and grow the smallest particles to sizes where they coagulate more slowly (increasing the predicted CN₁₀). In the binary nucleation cases, the former dominates, while in the ternary nucleation cases, the latter does.

As mentioned earlier, there are difficulties in comparing measurements from individual sites with grid-cell averaged concentrations. Similarly, it is possible that some scenarios compare well to observations because of compensating errors. Given these challenges and uncertainties, we avoid ruling out any of these scenarios as implausible. The rest of our analysis focuses on understanding the implications of different scenarios and processes explored here.

3.3 Nucleation with base-case present-day emissions

Figure 3 shows pressure-latitude maps of the annually averaged nucleation rates, CN₁₀ concentrations, and CCN(0.2%) concentrations for the BINARY and TERNARY simulations. Consistent with the global nucleation rates in Table 2, the nucleation rate in TERNARY is many orders of magnitude faster than in BINARY in panels (a) and (b). Furthermore, nucleation in TERNARY is ubiquitous throughout the troposphere (Fig. 3b), where in BINARY it is limited to colder altitudes and does not extend appreciably into the boundary layer (Fig. 3a). This implies that the model is predicting that free ammonia occurs, at least some of the time, throughout the entire troposphere. This is what is seen in Plate 3 of Adams et al. (1999), which our ammonia fields match closely. The nucleation rates shown here in Fig. 3a and b

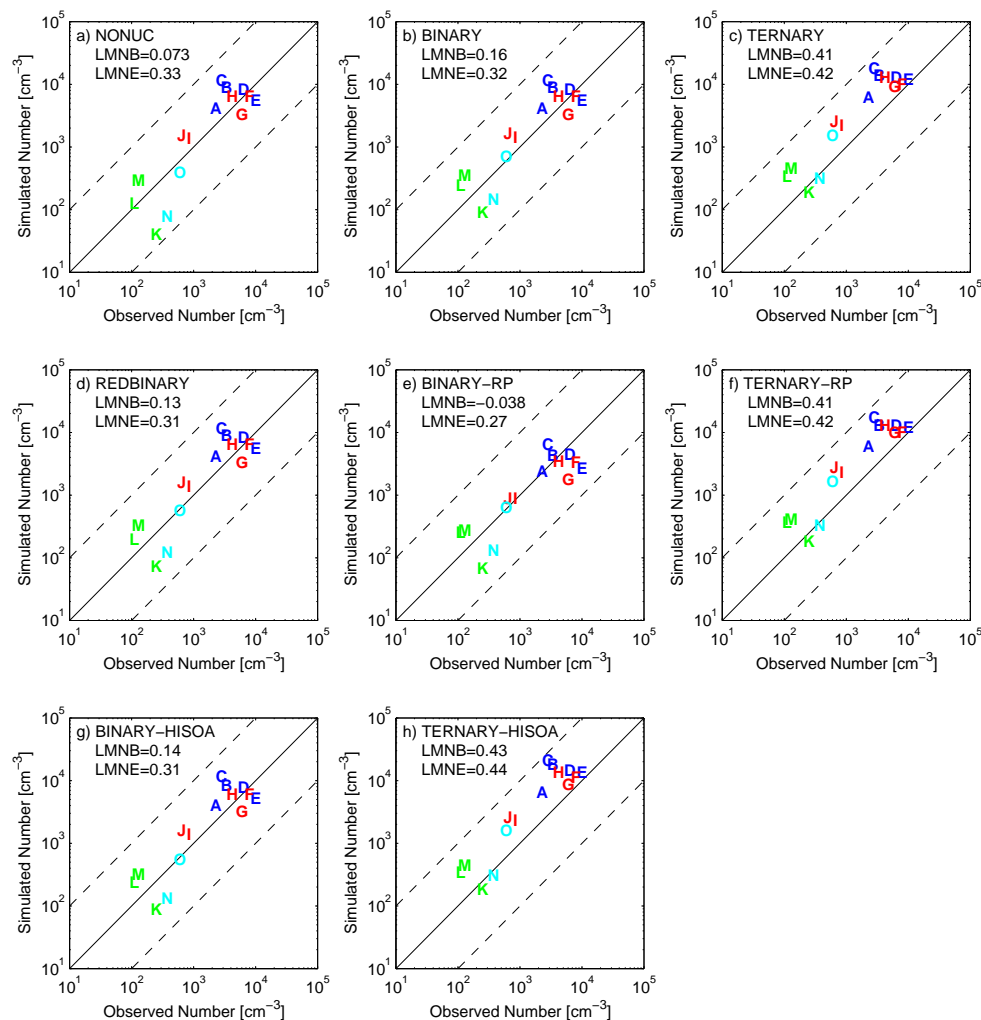


Fig. 2. Comparison of annually averaged predicted aerosol number concentration ($D_p > 10$ nm) to observations for the eight present-day simulations (cm^{-3} at 273 K and 1 atm). The locations are presented in Table 3 and Fig. 1. The solid line shows a 1:1 ratio and the dashed lines show ratios of 10:1 and 1:10. Dark blue letters denote European boundary layer, red letters denote North American polluted boundary layer, green letters denote remote boundary layer, and cyan letters denote free troposphere. Log-mean normalized bias (LMNB) and log-mean normalized error (LMNE) are given on each panel.

is qualitatively similar to the binary and ternary nucleation rates predicted by Lucas and Akimoto (2006) in their Fig. 2. As with the TERNARY simulation here, Lucas and Akimoto (2006) using Napari et al. (2002) predict ternary nucleation throughout the entire troposphere with annually averaged nucleation rates around $10^5 \text{ cm}^{-3} \text{ s}^{-1}$ throughout much of the atmosphere. The predictions of binary nucleation are also similar to the Lucas and Akimoto (2006) prediction using Vehkamäki et al. (2002); both show maximum nucleation rates predicted in the Northern Hemisphere free troposphere, lower nucleation rates in the southern hemisphere free troposphere and very little nucleation near the surface. The maximum nucleation rates in BINARY, however, appear to be one or two orders of magnitude lower than the binary nucleation rates predicted in Lucas and Akimoto (2006). A potential

reason for the difference in nucleation rates between these results and Lucas and Akimoto (2006) is that the aerosol fields in Lucas and Akimoto (2006) do not respond to nucleation events (Lucas and Prinn, 2003).

Regions of high nucleation in the TERNARY simulation show increases in CN10 over the BINARY simulations (Fig. 3c and d). The differences in CN10 concentrations are, however, much smaller than the differences in nucleation rates. As shown in Table 2, the CN10 globally are different by only a factor of about 2.5. The reasons for the reduced sensitivity of CN10 to changes in nucleation rate are similar to the dampening of changes in the new particle formation rate at 10 nm. Again, these reasons are a combination of slower condensational growth rates at faster nucleation rates due to larger condensational sinks, faster coagulation removal

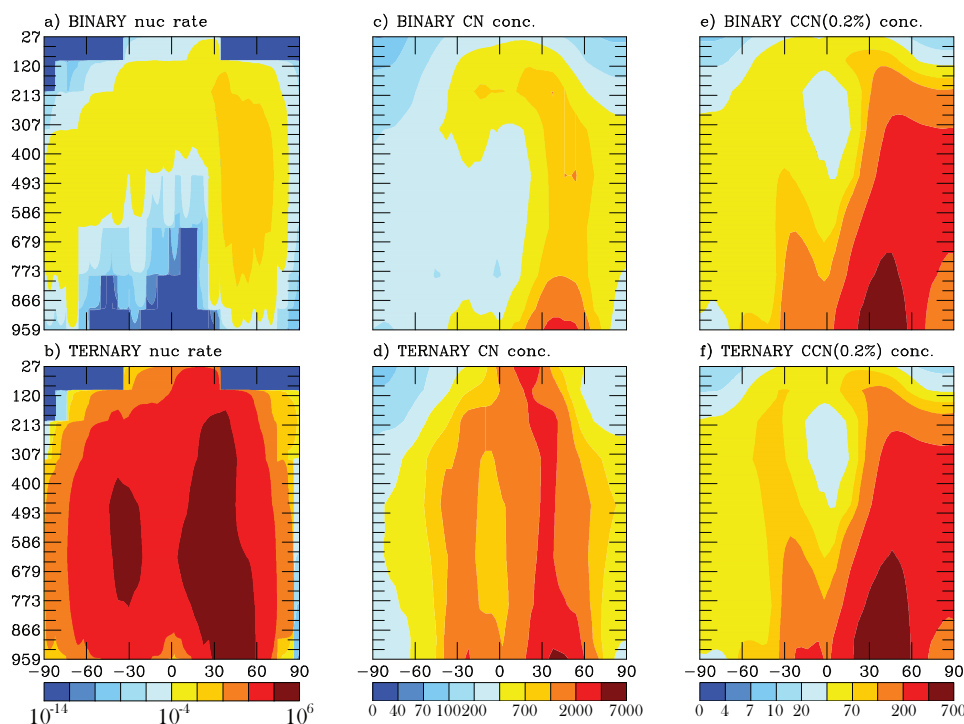


Fig. 3. Pressure (hPa) vs. latitude maps for annually averaged nucleation rates ($\text{cm}^{-3} \text{s}^{-1}$ at 273 K and 1 atm), CN ($D_p > 10 \text{ nm}$) (cm^{-3} at 273 K and 1 atm), CCN(0.2%) (cm^{-3} at 273 K and 1 atm) for the BINARY and TERNARY simulations.

rates at faster nucleation rates due to larger coagulation sinks and the lack of growth through nucleation-mode self coagulation in the Kerminen et al. (2004) parameterization.

The sensitivity of CCN(0.2%) to changes in nucleation (Fig. 3e and f) is even lower than the that of CN10 (Fig. 3c and d). This is because the nucleated particles that grew to 10 nm must now grow to sizes where they can act as CCN at 0.2% supersaturation ($D_p > \sim 80 \text{ nm}$). Because the Kerminen et al. (2004) parameterization is not used for the growth of these sized particles, the dampening is due to changes in the condensation and coagulation sinks with nucleation rate. The very low value of NUE in the TERNARY simulation shows that the tropospheric CCN system is reaching a saturation point with respect to new particle formation; insufficient condensable vapor exists to grow all these particles to CCN sizes. The ratio of the CCN(0.2%) for the TERNARY and BINARY simulations is shown in Fig. 4c. This shows that throughout most of the troposphere, the CCN(0.2%) concentrations increase by 5–20% when switching from binary to ternary nucleation. The global CCN burden in Table 2 increases by 17% when switching from binary to ternary nucleation. Although there are about 6 orders of magnitude more particles forming in the atmosphere in the TERNARY case, the effect on CCN is small because this increase in nucleation is nearly cancelled by the large decrease in the NUE (Table 2).

To assess the contribution of nucleation to CCN(0.2%), Fig. 4a shows the ratio of CCN(0.2%) predicted using the BINARY simulation to that of the NONUC simulation. The omission of nucleation in the model leads to large reductions of CCN(0.2%) in the upper troposphere with the CCN(0.2%) more than 50% larger when nucleation occurs. Towards the surface, primary emissions contribute more strongly to CCN(0.2%) and omission of nucleation changes the CCN(0.2%) less. Globally, the total CCN(0.2%) drops by only about 19% (Table 2) from the BINARY value when nucleation is omitted (percent changes near the surface are weighted more because the concentrations are higher). Figure 4b shows the ratio of CCN(0.2%) predicted using the BINARY simulation to that of the REDBINARY simulation. The effect of reducing the Vehkamäki et al. (2002) nucleation rates by a factor of ten has only a minor effect on the CCN(0.2%) concentrations. As shown in Table 2, the global nucleation rate in REDBINARY is 21% of the global nucleation rate in BINARY. Although the binary nucleation rate at constant sulfuric acid production is reduced to 10%, the global nucleation rate is still 21% of the original because of a feedback where the reduction in the nucleation rate causes the sulfuric acid vapor concentration to be larger, increasing the nucleation rate. Other reasons for the dampening of the changes in CCN(0.2%) to changes in the nucleation rate include the changes in the coagulation and condensation sinks with changes in the nucleation rate, similar to the comparison

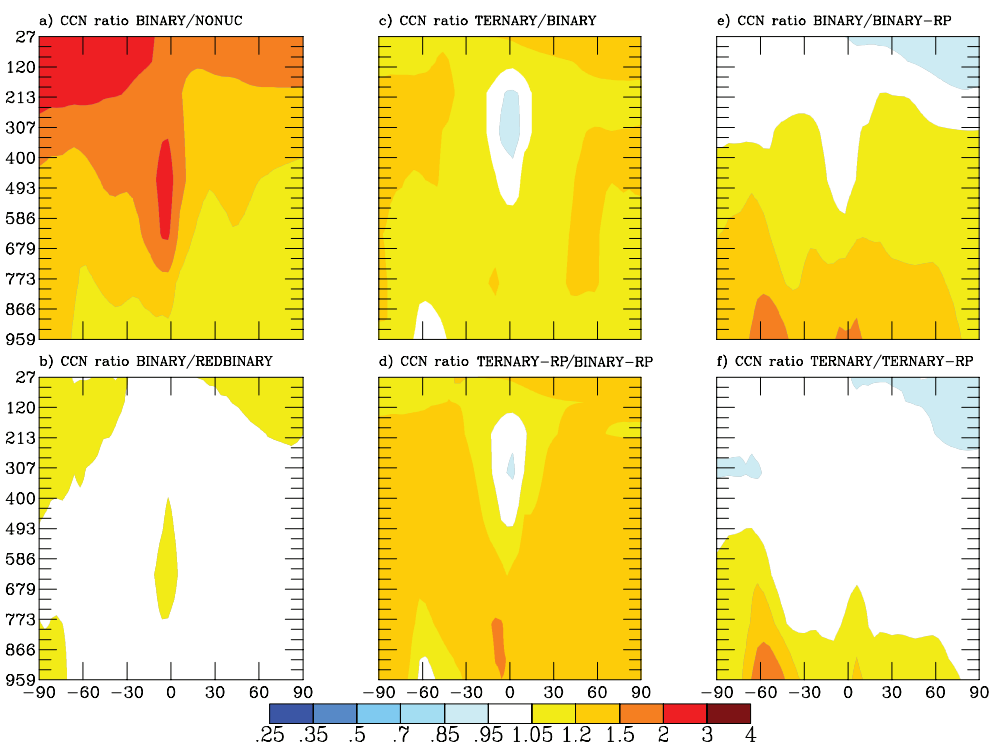


Fig. 4. Pressure (hPa) vs. latitude maps of the annually averaged ratios of CCN(0.2%) concentrations from the following scenarios: (a) BINARY to NONUC, (b) BINARY to REDBINARY, (c) TERNARY to BINARY, (d) TERNARY-RP to BINARY-RP, (e) BINARY to BINARY-RP, and (f) TERNARY to TERNARY-RP.

of BINARY and TERNARY. This dampening is reflected in the NUE values in Table 2. All else being equal, increasing the nucleation rate decreases the number utilization efficiency, the fraction of new particles that become CCN(0.2%).

Also shown in Table 2 is the effect of activation nucleation in the boundary layer on tropospheric CCN(0.2%). In June, the tropospheric-average nucleation in ACTIVATION is a factor of 10 higher than in BINARY causing an increase in CN10 by 17% across the troposphere. The global CCN(0.2%) increases by about 5%. As shown in Fig. 5, the boundary layer CCN(0.2%) also increase by 5% as tropospheric CCN(0.2%) are dominated by boundary layer CCN(0.2%). Figure 5b shows that the increase in boundary layer CCN(0.2%) from BINARY to TERNARY is more than twice that of Fig. 5a. If the nucleation rates in the TERNARY simulation are unrealistically high, this 5% sensitivity of CCN(0.2%) to nucleation between the ACTIVATION and BINARY simulations may be a more realistic bound for the sensitivity of CCN(0.2%) to nucleation for our base case emissions and SOA.

Across the 5 simulations with present-day base-case primary emissions and SOA, the CCN(0.2%) increases monotonically with increasing global nucleation rates between the NONUC, REDBINARY, BINARY, ACTIVATION and TERNARY simulations. For the reasonably comprehensive span of nucleation rates, mechanisms and distributions sam-

pled here, the global CCN(0.2%) appears to increase monotonically with increases in global nucleation albeit with diminishing return due to a decrease in NUE with increasing nucleation rate. We found only one example in which CCN(0.2%) decreased with increasing nucleation rate: the tropical upper troposphere (Fig. 4c and d). The reduction is modest (5–10%), localized and in response to a strong change in nucleation rates. This occurs because the very cold temperatures in this region favor nucleation even at low H_2SO_4 concentrations, concentrations too low to grow the nuclei efficiently to CCN sizes. This behavior is not observed in our simulations in the planetary boundary layer.

The 5% sensitivity of CCN(0.2%) to the addition of activation nucleation in the boundary layer (with $A=1 \times 10^{-6} \text{ s}^{-1}$) was also seen by Wang and Penner (2008) in their simulations that also included primary sulfate particle emissions. However, when they did not include the primary sulfate particles, the sensitivity of CCN(0.2%) to nucleation increased greatly. A higher sensitivity of CCN(0.2%) to boundary layer nucleation was also seen by Makkonen et al. (2008), who had on a small number emission rate of primary sulfate. The contrast of these results shows that the sensitivity of CCN(0.2%) to nucleation may depend greatly on the primary emissions rates. This sensitivity will be explored in more detail in the next section.

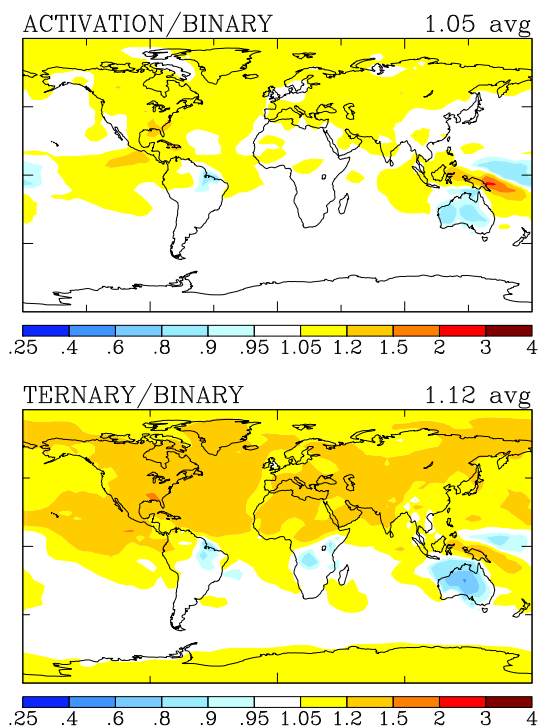


Fig. 5. Latitude versus longitude maps of the monthly average ratios of CCN(0.2%) concentrations for the month of June from the following scenarios: (a) ACTIVATION to BINARY and (b) TERNARY to BINARY.

3.4 Contribution of primary emissions to CCN

In this section, we explore both the sensitivity of CCN to changes in primary emissions rates as well as how the sensitivity of CCN to nucleation itself changes with primary emissions rates. Figure 4c shows the sensitivity of CCN(0.2%) to changes in the nucleation rate with the base-case present day emissions. Figure 4d shows this sensitivity when the primary aerosol emissions have been reduced by a factor of 3 (ratio of CCN(0.2%) in TERNARY-RP to BINARY-RP). As may be expected, with lower primary emissions, nucleation contributes a greater fraction of the CCN(0.2%) and nuclei have less competition for condensing vapors, so the CCN(0.2%) are thus more sensitive to the nucleation rate. Much of the free troposphere and tropical boundary layer in Fig. 4d shows CCN(0.2%) increases greater than 20%. Globally, there is a 33% increase in CCN(0.2%) between TERNARY-RP and BINARY-RP (Table 2) as compared to only a 17% increase for base-case primary emissions. This increase in sensitivity of CCN(0.2%) to nucleation with decreased primary emissions was also seen in Wang and Penner (2008). Figure 4e and f shows the sensitivity of CCN(0.2%) to changes in the primary emissions under binary (Fig. 4e) and ternary (Fig. 4f) nucleation. Both panels show that the CCN(0.2%) are most sensitive to the changes in the primary emissions rates in the lower atmo-

sphere and insensitive to primary emissions rates in the upper troposphere. The region most affected by changes in the emissions rate is the area around the Southern Ocean where sea-salt emissions of CCN sizes tend to dominate the CCN(0.2%). In the TERNARY/TERNARY-RP comparison in particular (Fig. 4f), the CCN(0.2%) is quite insensitive (<5%) to primary emissions throughout most of the free troposphere. The globally-averaged CCN(0.2%) increase from BINARY-RP to BINARY is 17%, whereas the CCN(0.2%) increase from TERNARY-RP to TERNARY is only 3%. This highlights that if nucleation rates are fast, as predicted by Napari et al. (2002), the CCN concentrations are insensitive to primary emissions throughout much of the troposphere (with the important exception of the boundary layer where CCN affect low level clouds). Although CCN(0.2%) is more sensitive to the nucleation rates in the reduced primary cases, the overall NUE is lower in these cases. This is because the primary emissions in general have a much higher probability of becoming a CCN, so the removal of the primary emissions lowers the overall NUE.

3.5 Sensitivity to SOA production rates

The high SOA simulations (HISOA) have SOA production rates over 3 times larger than in the base case simulations. The additional SOA is formed in polluted regions where anthropogenic SO₂ is emitted. Increasing the amount of condensable vapor increases the fraction of primary particles and nuclei that grow to CCN, as illustrated by the NUE values in Table 2. The HISOA scenarios have NUE values that are 30–50% higher than the corresponding base-case SOA simulations. Figure 6 illustrates how changes in the uncertain SOA production rates affect CCN(0.2%) as well as the sensitivity of CCN(0.2%) to the nucleation rates. Figure 6a shows the change in CCN(0.2%) when the additional SOA is added to the BINARY simulation. Figure 6b shows the change in CCN(0.2%) when the additional SOA is added to the TERNARY simulation. Figure 6c shows the sensitivity of CCN(0.2%) to nucleation rates when the additional SOA is present. Figure 6a and b show similar increases in CCN(0.2%) when the additional SOA is added. The increase is largest near the surface north of 30° N. This region corresponds to the areas where most of the “additional SOA” is produced in the model. The lifetime of the SOA precursor is only 12 h, so most of it will not travel far from the surface.

In Fig. 6c, the sensitivity of CCN(0.2%) to nucleation in these high SOA simulations is somewhat larger than this sensitivity in the base case simulations (Fig. 4c). This increase shows that with more SOA and faster condensational growth rates, the ternary nucleation simulations become more effective at growing nuclei to CCN sizes. This is similar to the enhancement of the contribution of nucleation to boundary layer CCN because of increased SOA condensation rates that was presented in Spracklen et al. (2008). The sensitivity of CCN(0.2%) to nucleation rates in Fig. 6c is somewhat

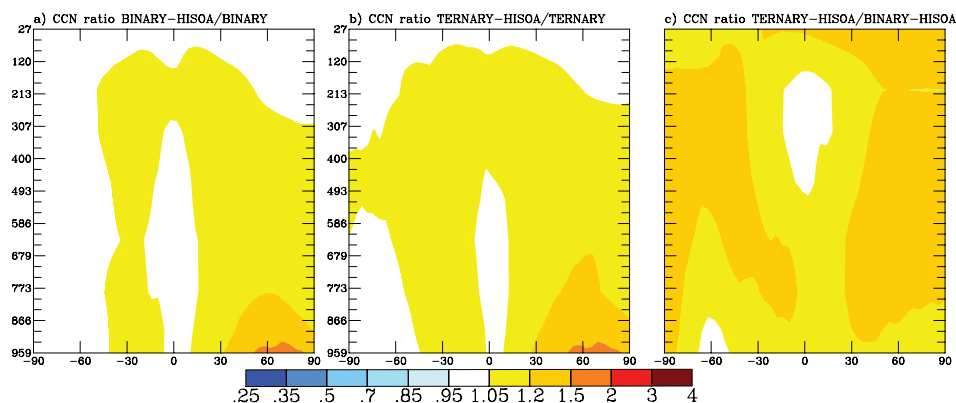


Fig. 6. Pressure (hPa) vs. latitude maps of the annually averaged ratios of CCN(0.2%) concentrations from the following scenarios: (a) BINARY-HISOA to BINARY, (b) TERNARY-HISOA to TERNARY and (c) TERNARY-HISOA to BINARY-HISOA.

smaller than this sensitivity in the reduced primary emissions simulations (Fig. 4d). The global sensitivities of CCN(0.2%) to nucleation rates are 17% in the base case simulations, 33% in the reduced primary emissions simulations and 20% in the high SOA simulations (Table 2). Although the simulations are not done here, we expect the CCN(0.2%) concentrations to be most sensitive to nucleation rates if both the reduced primary emissions and high SOA assumptions are considered simultaneously.

3.6 Pre-industrial simulations

In understanding the effect of changes in aerosols on clouds and climate, we are concerned with how CCN have changed between pre-industrial times and today. In this section, we explore the sensitivity of CCN(0.2%) to nucleation rates during pre-industrial times. This analysis will allow us to see if this sensitivity has changed since pre-industrial times, and it also allows us to see if the indirect forcing depends on the nucleation parameterization. Figure 7 shows pressure-latitude maps of the annually averaged nucleation rates, CN10 concentrations, and CCN(0.2%) concentrations for the BINARY-PI and TERNARY-PI simulations. The pre-industrial nucleation rates shown in Fig. 7a and b shows similar spatial trends to the present-day nucleation rates in Fig. 3a and b; however, the pre-industrial nucleation rates are a factor of 10 lower for binary nucleation and a factor of 5 lower for ternary nucleation (Table 2). The clear influence of primary emissions on the present-day CN10 in the lower troposphere (Fig. 3c and d) is not present in the pre-industrial CN10 (Fig. 7c and d) where nucleation is the dominant contributor to CN10 globally (Table 2). The CN10 in the Northern Hemisphere boundary layer in the TERNARY-PI are high due to the stronger source of ammonia in the Northern Hemisphere than in the southern hemisphere. The global sensitivity of CN10 to the nucleation rates is about a factor of 2.5 to 3 in the pre-industrial simulations, similar to the present-day base-case simulations.

To explore the sensitivity of pre-industrial CCN(0.2%) to the nucleation rate, Fig. 7e shows the CCN(0.2%) for the BINARY-PI case, Fig. 7f shows the CCN(0.2%) for the TERNARY-PI case, Figs. 8a and 8b show the changes in CCN(0.2%) between preindustrial times and today for binary and ternary nucleation, respectively, and Fig. 8c shows the ratio of CCN(0.2%) in the TERNARY-PI simulation to that in the BINARY-PI simulation. Qualitatively, this ratio plot (Fig. 8c) looks similar to the plot of CCN(0.2%) TERNARY:BINAR ratio (Fig. 4c). Globally, there is a 24% increase in CCN(0.2%) in the TERNARY-PI simulation over the BINARY-PI simulation, somewhat larger than the 17% increase between the TERNARY and BINARY simulations. There is, however, large uncertainty in the sensitivity of CCN(0.2%) to nucleation in the pre-industrial simulations due to large uncertainties in primary aerosol and precursor gas emissions. It is also worth noting that the NUE is higher in the pre-industrial simulations than in the present-day simulations. This may be due to either the reduced coagulation sink or a higher fraction of new particles being emissions at CCN sizes (e.g. sea salt) in the pre-industrial simulations.

Figure 8a and b show the changes in CCN(0.2%) between the pre-industrial simulations and the present-day base-case simulations when binary nucleation and ternary nucleation are used in the model, respectively. The change in CCN(0.2%) is large regardless of the nucleation parameterization used. The largest changes occur in the Northern Hemisphere where strong anthropogenic pollution is added in the present-day simulations. Globally averaged, the increase in CCN(0.2%) from pre-industrial times to the present day is 3.2 and 3.0 for binary and ternary, respectively (Table 2). To estimate the effect of uncertain nucleation rates on indirect forcing, we compare the boundary layer average CCN(0.2%) concentration between the pre-industrial simulations and the base-case present-day simulations. We use the boundary layer averages because low clouds have the greatest spatial coverage and are generally

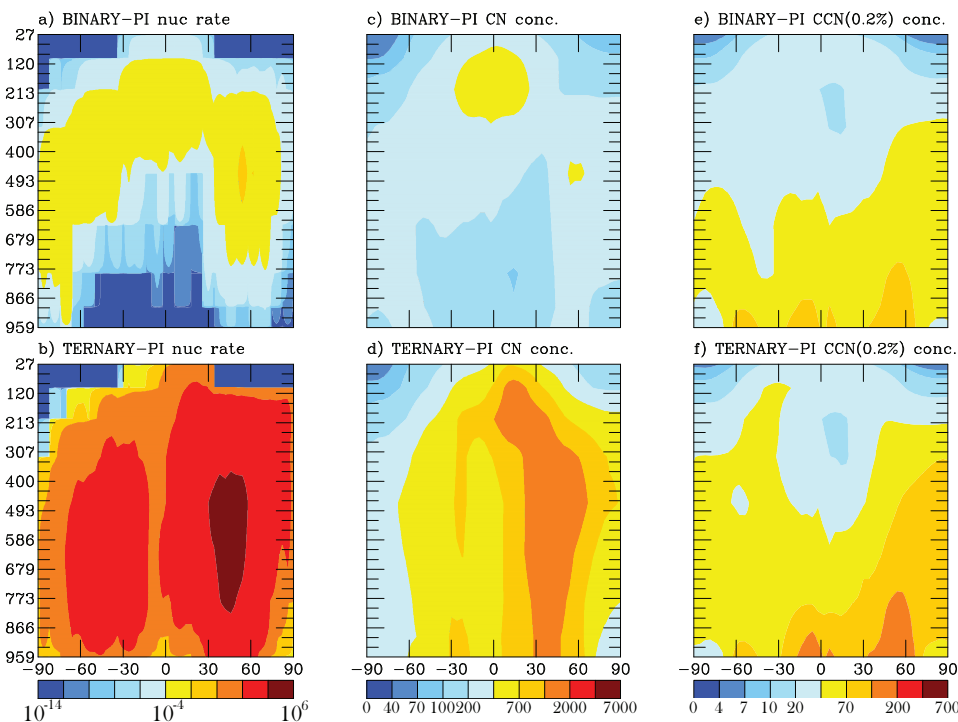


Fig. 7. Pressure (hPa) vs. latitude maps for annually averaged nucleation rates ($\text{cm}^{-3} \text{s}^{-1}$ at 273 K and 1 atm), CN ($D_p > 10 \text{ nm}$) (cm^{-3} at 273 K and 1 atm), CCN(0.2%) (cm^{-3} at 273 K and 1 atm) for the BINARY-PI and TERNARY-PI simulations.

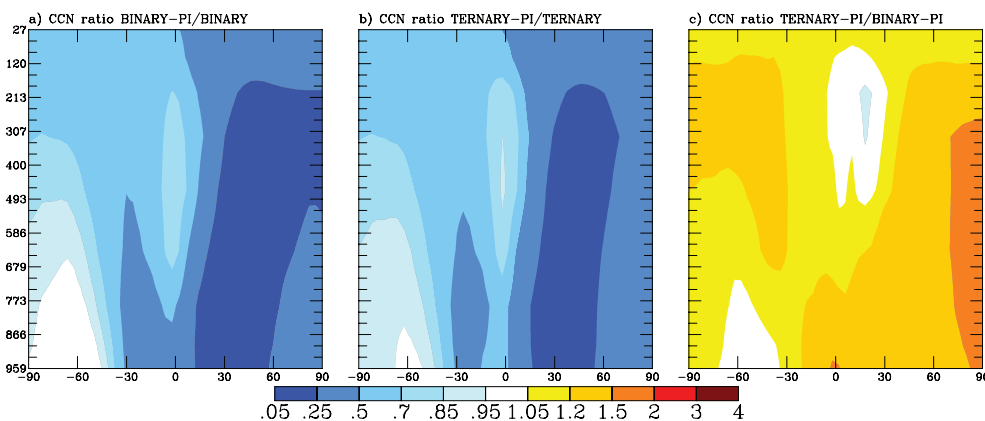


Fig. 8. Pressure (hPa) vs. latitude maps of the annually averaged ratios of CCN(0.2%) concentrations from the following scenarios: (a) BINARY-PI to BINARY, (b) TERNARY-PI to TERNARY and (c) TERNARY-PI to BINARY-PI.

thin and susceptible to changes in CCN concentrations. The boundary layer average CCN(0.2%) concentrations are 71.8, 92.0, 261 and 297 cm^{-3} for BINARY-PI, TERNARY-PI, BINARY and TERNARY simulations, respectively. If meteorology is held constant and cloud microphysical feedbacks are ignored, the change in cloud albedo is proportional to $\ln(\text{CCN}_{\text{present-day}}/\text{CCN}_{\text{pre-industrial}})$, which is 1.29 for the binary nucleation simulations and 1.17 for the ternary nucleation simulations. This rough calculation suggests that uncertain nucleation rates only contribute about 10% uncer-

tainty in the indirect effect between pre-industrial times and today. This suggests that the anthropogenic indirect forcing may not be sensitive to the nucleation mechanism; however, as shown in the previous sections, the effect of nucleation rate on present day CCN depends on primary emissions and SOA, which are both uncertain, so this insensitivity may be a coincidence. Nevertheless, it appears that the effects of increased primary emissions (tending to reduce the importance of nucleation) and the effects of increased condensable vapors (tending to increase the importance of nucleation)

largely cancel between pre-industrial and present-day simulations.

4 Conclusions

Uncertainties in nucleation and primary emissions affect our prediction of CCN and cloud radiative forcing. In this paper, we evaluated the uncertainty in CCN(0.2%) concentrations due to uncertainty in the nucleation and primary emission rates in a general circulation model with online size-resolved aerosol microphysics.

We found that large uncertainties in nucleation rates cause modest uncertainties in present-day CCN(0.2%) concentrations. Between two nucleation parameterizations, the binary nucleation parameterization of Vehkamäki et al. (2002) and the ternary nucleation parameterization of Napari et al. (2002), the nucleation rate varied by six orders of magnitude, globally. The number of present-day CCN(0.2%) increased by 17% in the troposphere and increased by 12% in the boundary layer when using Napari et al. (2002) rather than Vehkamäki et al. (2002). As evidenced by the very low values of the number utilization efficiency (NUE) in the TERNARY simulation, the tropospheric CCN system is has reached a saturation point at the very high nucleation rates, and only a very small fraction ($<10^{-7}$) of the particles can grow to CCN sizes. Using two additional nucleation schemes, one with reduced binary nucleation and another with cluster activation-type nucleation in the boundary layer, we found that global CCN monotonically increased with increasing global nucleation rates. This implies that although the CCN concentrations may saturate, the CCN concentration does not likely reach a maximum and then decrease with increasing nucleation rates (at least for the large range of nucleation rates tested here).

The sensitivity of CCN(0.2%) to changes in nucleation rate increased both when the primary particle emissions were reduced and when the SOA formation rates were increased. In simulations where all primary particle emissions were reduced by a factor of 3 (both number and mass), the sensitivity of CCN(0.2%) to nucleation was 33% globally averaged, about twice that of the base case primary emissions. In simulations where additional SOA was added to the biogenic SOA in the base case, increasing SOA by over a factor of 3, the sensitivity of CCN(0.2%) to nucleation was 20%, globally, slightly higher than that of base case SOA (17%). Because the primary particle emissions and SOA formation rates are uncertain globally, this shows that the relative contribution of nucleation to CCN depends very much on the availability of condensable vapor to grow the nuclei as well as competition from primary particulate emissions.

Uncertainty in CCN(0.2%) from uncertainty in primary emissions was as large as, if not larger than, the uncertainty in CCN(0.2%) from nucleation. As expected, nucleation is relatively more important to CN10 and CCN in the upper

troposphere while primary emissions were more important in the boundary layer. Primary emissions mass and number were scaled globally by a factor of 3 and the CCN(0.2%) varied by 17% in throughout the troposphere and by 40% in the boundary layer (when binary nucleation was used). The sensitivity of CCN(0.2%) to primary emissions were reduced when ternary nucleation is used (3% in the whole troposphere and 22% in the boundary layer); this shows that primary emissions are less important for generating CCN when nucleation rates are high. The number, mass and size of primary emissions must be better constrained in order to reduce uncertainty in CCN(0.2%).

Similar to present-day CCN(0.2%), pre-industrial CCN(0.2%) was also sensitive to the nucleation parameterization; however, the change in CCN between pre-industrial times and present day was less sensitive to the choice of nucleation parameterization. When the binary nucleation parameterization was used, CCN(0.2%) increased by a factor of 3.2 between the pre-industrial and present-day simulations. Similarly, when the ternary nucleation parameterization was used, CCN(0.2%) increased by a factor of 3.0. In the boundary layer, a rough estimate suggests that the sensitivity of the indirect effect (on albedo) to which nucleation parameterization is used is only $\sim 10\%$. However, because this result depends on a cancellation of the effects of anthropogenic primary emissions (increasing the condensation and coagulation sinks, thus reducing the effect of nucleation) and anthropogenic condensable vapor (increasing the effect of nucleation), this insensitivity may be partly coincidental.

Uncertainties in nucleation, primary emissions and SOA may all affect predictions of CCN. Other than the small effect of the nucleation rate parameterization on the change in CCN from pre-industrial times to today, which may be coincidental, the results herein showed that significant work must be done to reduce the uncertainties in these processes before we may better understand the aerosol indirect effect. Furthermore, we did not specifically address the changes in CCN to changes in the primary emission size distribution while keeping the primary mass emissions rates constant, and this will contribute to additional uncertainty in CCN from primary emissions.

Acknowledgements. This research was supported by the Environmental Protection Agency (EPA) through the Science to Achieve Results (STAR) Graduate Fellowship (91668201-0) as well as a research grant from the National Aeronautics and Space Administration (NASA grant NNG04GE86G).

Edited by: A. Laaksonen

References

- Ackerman, A. S., Kirkpatrick, M. P., Stevens, D. E., and Toon, O. B.: The impact of humidity above stratiform clouds on indirect aerosol climate forcing, *Nature*, 432, 1014–1017, 2004.
- Adams, P. J. and Seinfeld, J. H.: Disproportionate impact of particulate emissions on global cloud condensation nuclei concentrations, *Geophys. Res. Lett.*, 30, 1239, doi:10.1029/2002GL016303, 2003.
- Adams, P. J. and Seinfeld, J. H.: Predicting global aerosol size distributions in general circulation models, *J. Geophys. Res.*, 107, 4370, doi:10.1029/2001JD001010, 2002.
- Adams, P. J., Seinfeld, J. H., Koch, D., Mickley, L., and Jacob, D.: General circulation model assessment of direct radiative forcing by the sulfate-nitrate-ammonium- water inorganic system, *J. Geophys. Res.*, 106, 1097–1111, 2001.
- Adams, P. J., Seinfeld, J. H., and Koch, D. M.: Global concentrations of tropospheric sulphate, nitrate, and ammonium aerosols simulated in a general circulation model, *J. Geophys. Res.*, 104, 13 791–13 823, 1999.
- Albrecht, B. A.: Aerosols, Cloud Microphysics, and Fractional Cloudiness, *Science*, 245, 1227–1230, 1989.
- Anttila, T., Vehkamäki, H., Napari, I., and Kulmala, M.: Effect of ammonium bisulphate formation on atmospheric water-sulphuric acid-ammonia nucleation, *Boreal Environ. Res.*, 10, 511–523, 2005.
- Bond, T. C., Streets, D. G., Yarber, K. F., Nelson, S. M., Woo, J. H., and Klimont, Z.: A technology-based global inventory of black and organic carbon emissions from combustion, *J. Geophys. Res.*, 109, D14203, doi:10.1029/2003JD003697, 2004.
- Bouwman, A. F., Lee, D. S., Asman, W. A. H., Dentener, F. J., VanderHoek, K. W., and Olivier, J. G. J.: A global high-resolution emission inventory for ammonia, *Global Biogeochem. Cy.*, 11, 561–587, 1997.
- Clarke, A. D., Owens, S. R., and Zhou, J. C.: An ultrafine sea-salt flux from breaking waves: Implications for cloud condensation nuclei in the remote marine atmosphere, *J. Geophys. Res.*, 111, D06202, doi:10.1029/2005JD006565, 2006.
- Del Genio, A. D. and Yao, M.-S.: Efficient Cumulus Parameterization for Long-Term Climate Studies: The GISS Scheme, *Meteorol. Monogr.*, 24, 181–184, 1992.
- Del Genio, A. D., Yao, M.-S., Kovari, W., and Lo, K.: A Prognostic Cloud Water Parameterization for Global Models, *J. Climate*, 9, 270–304, 1996.
- Dentener, F., Kinne, S., Bond, T., Boucher, O., Cofala, J., Generoso, S., Ginoux, P., Gong, S., Hoelzemann, J. J., Ito, A., Marelli, L., Penner, J. E., Putaud, J. P., Textor, C., Schulz, M., van der Werf, G. R., and Wilson, J.: Emissions of primary aerosol and precursor gases in the years 2000 and 1750 prescribed data-sets for AeroCom, *Atmos. Chem. Phys.*, 6, 4321–4344, 2006, <http://www.atmos-chem-phys.net/6/4321/2006/>.
- Easter, R. C., Ghan, S. J., Zhang, Y., Saylor, R. D., Chapman, E. G., Laulainen, N. S., Abdul-Razzak, H., Leung, L. R., Bian, X. D., and Zaveri, R. A.: MIRAGE: Model description and evaluation of aerosols and trace gases, *J. Geophys. Res.*, 109, D20210, doi:10.1029/2004JD004571, 2004.
- El-Zanan, H. S., Lowenthal, D. H., Zielinska, B., Chow, J. C., and Kumar, N.: Determination of the organic aerosol mass to organic carbon ratio in IMPROVE samples, *Chemosphere*, 60, 485–496, 2005.
- Fan, J. W., Zhang, R. Y., Collins, D., and Li, G. H.: Contribution of secondary condensable organics to new particle formation: A case study in Houston, Texas, *Geophys. Res. Lett.*, 33, L15802, doi:10.1029/2006GL026295, 2006.
- Forster, P., Ramaswamy, V., Artaxo, P., Berntsen, T., Betts, R., Fahey, D. W., Haywood, J., Lean, J., Lowe, D. C., Myhre, G., Nganga, J., Prinn, R., Raga, G., Schulz, M., and Dorland, R. V.: Changes in Atmospheric Constituents and in Radiative Forcing, in: *Climate Change 2007: The Physical Science Basis, Contribution of Working Group I to the Fourth Assessment Report of the Intergovernmental Panel on Climate Change*, edited by: Miller, H. L., Cambridge University Press, Cambridge, UK and New York, NY, USA, 129–234, 2007.
- Gaydos, T. M., Stanier, C. O., and Pandis, S. N.: Modeling of in situ ultrafine atmospheric particle formation in the eastern United States, *J. Geophys. Res.*, 110, D07S12, doi:10.1029/2004JD004683, 2005.
- Ghan, S. J., Easter, R. C., Chapman, E. G., Abdul-Razzak, H., Zhang, Y., Leung, L. R., Laulainen, N. S., Saylor, R. D., and Zaveri, R. A.: A physically based estimate of radiative forcing by anthropogenic sulfate aerosol, *J. Geophys. Res.*, 106, 5279–5293, 2001.
- Hansen, J., Russell, G., Rind, D., Stone, P., Lacis, A., Lebedeff, S., Ruedy, R., and Travis, L.: Efficient 3-Dimensional Global-Models for Climate Studies – Model-I and Model-II, *Mon. Weather Rev.*, 111, 609–662, 1983.
- Holmes, N. S.: A review of particle formation events and growth in the atmosphere in the various environments and discussion of mechanistic implications, *Atmos. Environ.*, 41, 2183–2201, 2007.
- Jacker-Voirol, A. and Mirabel, P.: Heteromolecular Nucleation in the Sulfuric Acid-Water System, *Atmos. Environ.*, 23, 2053–2057, 1989.
- Jung, J.: Regional air quality – Atmospheric nucleation interactions, Carnegie Mellon University, Pittsburgh, PA, USA, 2008.
- Jung, J. G., Adams, P. J., and Pandis, S. N.: Evaluation of nucleation theories in a sulfur-rich environment, in press, *Atmos. Environ.*, 2008.
- Jung, J. G., Adams, P. J., and Pandis, S. N.: Simulating the size distribution and chemical composition of ultrafine particles during nucleation events, *Atmos. Environ.*, 40, 2248–2259, 2006.
- Kanakidou, M., Seinfeld, J. H., Pandis, S. N., Barnes, I., Dentener, F. J., Facchini, M. C., Van Dingenen, R., Ervens, B., Nenes, A., Nielsen, C. J., Swietlicki, E., Putaud, J. P., Balkanski, Y., Fuzzi, S., Horth, J., Moortgat, G. K., Winterhalter, R., Myhre, C. E. L., Tsigaridis, K., Vignati, E., Stephanou, E. G., and Wilson, J.: Organic aerosol and global climate modelling: a review, *Atmos. Chem. Phys.*, 5, 1053–1123, 2005.
- Kazil, J. and Lovejoy, E. R.: Tropospheric ionization and aerosol production: A model study, *J. Geophys. Res.*, 109, D19206, doi:10.1029/2004JD004852, 2004.
- Kazil, J., Lovejoy, E. R., Barth, M. C., and O'Brien, K.: Aerosol nucleation over oceans and the role of galactic cosmic rays, *Atmos. Chem. Phys.*, 6, 4905–4924, 2006, <http://www.atmos-chem-phys.net/6/4905/2006/>.
- Kerminen, V. M., Anttila, T., Lehtinen, K. E. J., and Kulmala, M.: Parameterization for atmospheric new-particle formation: Application to a system involving sulfuric acid and condensable water-soluble organic vapors, *Aerosol Sci. Technol.*, 38, 1001–1008, 2009.

- 2004.
- Koch, D., Jacob, D., Tegen, I., Rind, D., and Chin, M.: Tropospheric sulfur simulation and sulfate direct radiative forcing in the Goddard Institute for Space Studies general circulation model, *J. Geophys. Res.*, 104, 23 799–23 822, 1999.
- Kulmala, M., Korhonen, P., Napari, I., Karlsson, A., Berresheim, H., and O’Dowd, C. D.: Aerosol formation during PARFORCE: Ternary nucleation of H₂SO₄, NH₃, and H₂O, *J. Geophys. Res.*, 107, 8111, doi:10.1029/2001JD000900, 2002.
- Kulmala, M., Laaksonen, A., and Pirjola, L.: Parameterizations for sulfuric acid/water nucleation rates, *J. Geophys. Res.*, 103, 8301–8307, 1998.
- Kulmala, M., Lehtinen, K. E. J., and Laaksonen, A.: Cluster activation theory as an explanation of the linear dependence between formation rate of 3nm particles and sulphuric acid concentration, *Atmos. Chem. Phys.*, 6, 787–793, 2006, <http://www.atmos-chem-phys.net/6/787/2006/>.
- Kulmala, M., Petaja, T., Monkkonen, P., Koponen, I. K., Dal Maso, M., Aalto, P. P., Lehtinen, K. E. J., and Kerminen, V. M.: On the growth of nucleation mode particles: source rates of condensable vapor in polluted and clean environments, *Atmos. Chem. Phys.*, 5, 409–416, 2005, <http://www.atmos-chem-phys.net/5/409/2005/>.
- Laakso, L., Makela, J. M., Pirjola, L., and Kulmala, M.: Model studies on ion-induced nucleation in the atmosphere, *J. Geophys. Res.*, 107, 4427, doi:10.1029/2002JD002140, 2002.
- Laaksonen, A., Hamed, A., Joutsensaari, J., Hiltunen, L., Cavalli, F., Junkermann, W., Asmi, A., Fuzzi, S., and Facchini, M. C.: Cloud condensation nucleus production from nucleation events at a highly polluted region, *Geophys. Res. Lett.*, 32, L06812, doi:10.1029/2004GL022092, 2005.
- Laaksonen, A., Kulmala, M., O’Dowd, C. D., Joutsensaari, J., Vaattovaara, P., Mikkonen, S., Lehtinen, K. E. J., Sogacheva, L., Dal Maso, M., Aalto, P., Petj, T., Sogachev, A., Yoon, Y. J., Lihavainen, H., Nilsson, D., Facchini, M. C., Cavalli, F., Fuzzi, S., Hoffmann, T., Arnold, F., Hanke, M., Sellegri, K., Umann, B., Junkermann, W., Coe, H., Allan, J. D., Alfarra, M. R., Worsnop, D. R., Riekkola, M.-L., Hyötyläinen, T., and Viisanen, Y.: The role of VOC oxidation products in continental new particle formation, *Atmos. Chem. Phys.*, 8, 2657–2665, 2008, <http://www.atmos-chem-phys.net/8/2657/2008/>.
- Lihavainen, H., Kerminen, V. M., Komppula, M., Hatakka, J., Aaltonen, V., Kulmala, M., and Viisanen, Y.: Production of “potential” cloud condensation nuclei associated with atmospheric new-particle formation in northern Finland, *J. Geophys. Res.*, 108, 4782, doi:10.1029/2003JD003887, 2003.
- Liou, C., Penner, J. E., Chuang, C., Walton, J. J., Eddleman, H., and Cachier, H.: A global three-dimensional model study of carbonaceous aerosols, *J. Geophys. Res.*, 101, 19 411–19 432, 1996.
- Lovejoy, E. R., Curtius, J., and Froyd, K. D.: Atmospheric ion-induced nucleation of sulfuric acid and water, *J. Geophys. Res.*, 109, D08204, doi:10.1029/2003JD004460, 2004.
- Lucas, D. D. and Akimoto, H.: Evaluating aerosol nucleation parameterizations in a global atmospheric model, *Geophys. Res. Lett.*, 33, L10808, doi:10.1029/2006GL025672, 2006.
- Lucas, D. D. and Prinn, R. G.: Tropospheric distributions of sulfuric acid-water vapor aerosol nucleation rates from dimethylsulfide oxidation, *Geophys. Res. Lett.*, 30, 2136, doi:10.1029/2003GL018370, 2003.
- Makkonen, R., Asmi, A., Korhonen, H., Kokkola, H., Järvenoja, S., Räisänen, P., Lehtinen, K. E. J., Laaksonen, A., Kerminen, V.-M., Järvinen, H., Lohmann, U., Feichter, J., Kulmala, M.: Sensitivity of aerosol concentrations and cloud properties to nucleation and secondary organic distribution in echam5-ham global circulation model, *Atmos. Chem. Phys. Discuss.*, 8, 10955–10998, 2008, <http://www.atmos-chem-phys-discuss.net/8/10955/2008/>.
- Merikanto, J., Napari, I., Vehkamäki, H., Anttila, T., and Kulmala, M.: New parameterization of sulfuric acid-ammonia-water ternary nucleation rates at tropospheric conditions, *J. Geophys. Res.*, 112, D15207, doi:10.1029/2006JD007977, 2007.
- Modgil, M. S., Kumar, S., Tripathi, S. N., and Lovejoy, E. R.: A parameterization of ion-induced nucleation of sulphuric acid and water for atmospheric conditions, *J. Geophys. Res.*, 110, D19205, doi:10.1029/2004JD005475, 2005.
- Napari, I., Noppel, M., Vehkamäki, H., and Kulmala, M.: Parametrization of ternary nucleation rates for H₂SO₄-NH₃-H₂O vapors, *J. Geophys. Res.*, 107, 4381, doi:10.1029/2002JD002132, 2002.
- Penner, J., Andreae, M. O., Annegarn, H., Barrie, L. A., Feichter, J., Hegg, D., Jayaraman, A., Leaitch, R., Murphy, D. M., Nganga, J., and Pitari, G.: Aerosols, their direct and indirect effects, in: *Climate Change 2001: The Science Basis*, edited by: Nyenzi, B. and Prospero, J. M., Cambridge University Press, Cambridge, United Kingdom and New York, NY, USA, 289–348, 2001.
- Pierce, J. R. and Adams, P. J.: Efficiency of cloud condensation nuclei formation from ultrafine particles, *Atmos. Chem. Phys.*, 7, 1367–1379, 2007, <http://www.atmos-chem-phys.net/7/1367/2007/>.
- Pierce, J. R. and Adams, P. J.: Global evaluation of CCN formation by direct emission of sea salt and growth of ultrafine sea salt, *J. Geophys. Res.*, 111, D06203, doi:10.1029/2005JD006186, 2006.
- Pierce, J. R., Chen, K., and Adams, P. J.: Contribution of primary carbonaceous aerosol to cloud condensation nuclei: processes and uncertainties evaluated with a global aerosol microphysics model, *Atmos. Chem. Phys.*, 7, 5447–5466, 2007, <http://www.atmos-chem-phys.net/7/5447/2007/>.
- Pierce, J. R., Theodoritsi, G., Adams, P. J., and Pandis, S. N.: Parameterization of the effect of sub-grid scale aerosol dynamics on aerosol number emission rates, *J. Aerosol Sci.*, in press, 2008.
- Pierce, J. R. and Adams, P. J.: A Computationally Efficient Aerosol Nucleation/Condensation Method: Pseudo-Steady-State Sulfuric Acid, *Aerosol Sci. Technol.*, 43, 1–11, 2009.
- Pirjola, L., O’Dowd, C. D., and Kulmala, M.: A model prediction of the yield of cloud condensation nuclei from coastal nucleation events, *J. Geophys. Res.*, 107, 8098, doi:10.1029/2000JD000213, 2002.
- Prather, M. J.: Numerical advection by conservation of second-order moments, *J. Geophys. Res.*, 91, 6671–6681, 1986.
- Raymond, T. M. and Pandis, S. N.: Cloud activation of single-component organic aerosols, *J. Geophys. Res.*, 107, 4787–4784, 2002.
- Raymond, T. M. and Pandis, S. N.: Formation of cloud droplets by multicomponent organic particles, *J. Geophys. Res.*, 108, 4469–4476, 2003.
- Rind, D. and Lerner, J.: Use of on-line tracers as a diagnostic tool in general circulation model development – 1.: Horizontal and ver-

- tical transport in the troposphere, *J. Geophys. Res.*, 101, 12 667–12 683, 1996.
- Rissler, J., Swietlicki, E., Zhou, J., Roberts, G., Andreae, M. O., Gatti, L. V., and Artaxo, P.: Physical properties of the sub-micrometer aerosol over the Amazon rain forest during the wet-to-dry season transition - comparison of modeled and measured CCN concentrations, *Atmos. Chem. Phys.*, 4, 2119–2143, 2004, <http://www.atmos-chem-phys.net/4/2119/2004/>.
- Rissler, J., Vestin, A., Swietlicki, E., Fisch, G., Zhou, J., Artaxo, P., and Andreae, M. O.: Size distribution and hygroscopic properties of aerosol particles from dry-season biomass burning in Amazonia, *Atmos. Chem. Phys.*, 6, 471–491, 2006, <http://www.atmos-chem-phys.net/6/471/2006/>.
- Rodriguez, M. A. and Dabdub, D.: A modeling study of size- and chemically resolved aerosol thermodynamics in a global chemical transport model, *J. Geophys. Res.*, 109, D02203, doi:10.1029/2003JD003639, 2004.
- Schnell, R. C.: Chapter 3: Aerosols and Radiation, in: *Climate Monitoring and Diagnostics Laboratory Summary Report No. 27 2002–2003*, edited by: McComisky, A., 2003.
- Sotiropoulou, R. E. P., Tagaris, E., Pilinis, C., Anttila, T., and Kulmala, M.: Modeling new particle formation during air pollution episodes: Impacts on aerosol and cloud condensation nuclei, *Aerosol Sci. Technol.*, 40, 557–572, 2006.
- Sihto, S.-L., Kulmala, M., Kerminen, V.-M., Dal Maso, M., Petaja, T., Riipinen, I., Korhonen, H., Arnold, F., Janson, R., Boy, M., Laaksonen, A., Lehtinen, K. E. J.: Atmospheric sulphuric acid and aerosol formation: implications from atmospheric measurements for nucleation and early growth mechanisms, *Atmos. Chem. Phys.*, 6, 4079–4091, 2006.
- Spracklen, D. V., Carslaw, K. S., Kulmala, M., Kerminen, V. M., Mann, G. W., and Sihto, S. L.: The contribution of boundary layer nucleation events to total particle concentrations on regional and global scales, *Atmos. Chem. Phys.*, 6, 5631–5648, 2006, <http://www.atmos-chem-phys.net/6/5631/2006/>.
- Spracklen, D. V., Carslaw, K. S., Kulmala, M., Kerminen, V. M., Sihto, S. L., Riipinen, I., Merikanto, J., Mann, G. W., Chipperfield, M. P., Wiedensohler, A., Birmili, W., and Lihavainen, H.: Contribution of particle formation to global cloud condensation nuclei concentrations, *Geophys. Res. Lett.*, 35, L16808, doi:10.1029/2007GL033038, 2008.
- Spracklen, D. V., Pringle, K. J., Carslaw, K. S., Chipperfield, M. P., and Mann, G. W.: A global off-line model of size-resolved aerosol microphysics: I. Model development and prediction of aerosol properties, *Atmos. Chem. Phys.*, 5, 2227–2252, 2005, <http://www.atmos-chem-phys.net/5/2227/2005/>.
- Spracklen, D. V., Pringle, K. J., Carslaw, K. S., Chipperfield, M. P., and Mann, G. W.: A global off-line model of size-resolved aerosol microphysics: II. Identification of key uncertainties, *Atmos. Chem. Phys.*, 5, 3233–3250, 2005, <http://www.atmos-chem-phys.net/5/3233/2005/>.
- Stier, P., Feichter, J., Kinne, S., Kloster, S., Vignati, E., Wilson, J., Ganzeveld, L., Tegen, I., Werner, M., Balkanski, Y., Schulz, M., Boucher, O., Minikin, A., and Petzold, A.: The aerosol-climate model ECHAM5-HAM, *Atmos. Chem. Phys.*, 5, 1125–1156, 2005, <http://www.atmos-chem-phys.net/5/1125/2005/>.
- Stier, P., Feichter, J., Roeckner, E., Kloster, S., and Esch, M.: Emission-induced nonlinearities in the global aerosol system, *J. Climate*, 19, 3845–3862, 2006.
- Twohy, C. H., Petters, M. D., Snider, J. R., Stevens, B., Tahnk, W., Wetzel, M., Russell, L., and Burnet, F.: Evaluation of the aerosol indirect effect in marine stratocumulus clouds: Droplet number, size, liquid water path, and radiative impact, *J. Geophys. Res.*, 110, D08203, doi:10.1029/2004JD005116, 2005.
- Twomey, S.: Aerosols, Clouds, and Radiation, *Atmos. Environ.*, 25A, 2435–2442, 1991.
- Twomey, S.: The Influence of Pollution on the Shortwave Albedo of Clouds, *J. Atmos. Sci.*, 34, 1149–1152, 1977.
- Twomey, S.: Pollution and the Planetary Albedo, *Atmos. Environ.*, 8, 1251–1256, 1974.
- Vaattovaara, P., Huttunen, P. E., Yoon, Y. J., Joutsensaari, J., Lehtinen, K. E. J., O'Dowd, C. D., and Laaksonen, A.: The composition of nucleation and Aitken modes particles during coastal nucleation events: evidence for marine secondary organic contribution, *Atmos. Chem. Phys.*, 6, 4601–4616, 2006, <http://www.atmos-chem-phys.net/6/4601/2006/>.
- Van Dingenen, R., Raes, F., Putaud, J. P., Baltensperger, U., Charon, A., Facchini, M. C., Decesari, S., Fuzzi, S., Gehrig, R., Hansson, H. C., Harrison, R. M., Hüglin, C., Jones, A. M., Laj, P., Lorbeer, G., Maenhaut, W., Palmgren, F., Querol, X., Rodriguez, S., Schneider, J., ten Brink, H., Tunved, P., Tørseth, K., Wehner, B., Weingartner, E., Wiedensohler, A., and Wahlin, P.: A European aerosol phenomenology – 1: physical characteristics of particulate matter at kerbside, urban, rural and background sites in Europe, *Atmos. Environ.*, 38, 2561–2577, 2004.
- Vehkamäki, H., Kulmala, M., Napari, I., Lehtinen, K. E. J., Timmerack, C., Noppel, M., and Laaksonen, A.: An improved parameterization for sulfuric acid-water nucleation rates for tropospheric and stratospheric conditions, *J. Geophys. Res.*, 107, 4622, doi:10.1029/2002JD002184, 2002.
- Wang, M. and Penner, J. E.: Aerosol indirect forcing in a global model with particle nucleation, *Atmos. Chem. Phys.*, 9, 239–260, 2009, <http://www.atmos-chem-phys.net/9/239/2009/>.
- Wilson, J., Cuvelier, C., and Raes, F.: A modeling study of global mixed aerosol fields, *J. Geophys. Res.*, 106, 34 081–34 108, 2001.
- Yu, F.: From molecular clusters to nanoparticles: second-generation ion-mediated nucleation model, *Atmos. Chem. Phys.*, 6, 5193–5211, 2006a, <http://www.atmos-chem-phys.net/6/5193/2006/>.
- Yu, F. Q.: Effect of ammonia on new particle formation: A kinetic H₂SO₄-H₂O-NH₃ nucleation model constrained by laboratory measurements, *J. Geophys. Res.*, 111, D01204, doi:10.1029/2005JD005968, 2006b.
- Yu, F. Q. and Turco, R. P.: From molecular clusters to nanoparticles: Role of ambient ionization in tropospheric aerosol formation, *J. Geophys. Res.*, 106, 4797–4814, 2001.
- Yu, L. E., Shulman, M. L., Kopperud, R., and Hildemann, L. M.: Fine organic aerosols collected in a humid, rural location (Great Smoky Mountains, Tennessee, USA): Chemical and temporal characteristics, *Atmos. Environ.*, 39, 6037–6050, 2005.
- Zhang, Q., Worsnop, D. R., Canagaratna, M. R., and Jimenez, J. L.: Hydrocarbon-like and oxygenated organic aerosols in Pittsburgh: insights into sources and processes of organic aerosols, *Atmos. Chem. Phys.*, 5, 3289–3311, 2005, <http://www.atmos-chem-phys.net/5/3289/2005/>.